Validation of a New Model-Based Tracking Technique for Measuring Three-Dimensional, In Vivo Glenohumeral Joint Kinematics

Michael J. Bey
e-mail: bey@bjc.hfh.edu

Roger Zauel

Stephanie K. Brock

Scott Tashman

Henry Ford Health Systems,
Department of Orthopaedics and Rehabilitation,
Bone and Joint Center, E&R 2015,
2799 W. Grand Blvd., Detroit, MI 48202

Shoulder motion is complex and significant research efforts have focused on measuring glenohumeral joint motion. Unfortunately, conventional motion measurement techniques are unable to measure glenohumeral joint kinematics during dynamic shoulder motion to clinically significant levels of accuracy. The purpose of this study was to validate the accuracy of a new model-based tracking technique for measuring three-dimensional, in vivo glenohumeral joint kinematics. We have developed a model-based tracking technique for accurately measuring in vivo joint motion from biplane radiographic images that tracks the position of bones based on their three-dimensional shape and texture. To validate this technique, we implanted tantalum beads into the humerus and scapula of both shoulders from three cadaver specimens and then recorded biplane radiographic images of the shoulder while manually moving each specimen's arm. The position of the humerus and scapula were measured using the model-based tracking system and with a previously validated dynamic radiostereometric analysis (RSA) technique. Accuracy was reported in terms of measurement bias, measurement precision, and overall dynamic accuracy by comparing the model-based tracking results to the dynamic RSA results. The model-based tracking technique produced results that were in excellent agreement with the RSA technique. Measurement bias ranged from −0.126 to 0.199 mm for the scapula and ranged from −0.022 to 0.079 mm for the humerus. Dynamic measurement precision was better than 0.130 mm for the scapula and 0.095 mm for the humerus. Overall dynamic accuracy indicated that rms errors in any one direction were less than 0.385 mm for the scapula and less than 0.374 mm for the humerus. These errors correspond to rotational inaccuracies of approximately 0.25 deg for the scapula and 0.47 deg for the humerus. This new model-based tracking approach represents a non-invasive technique for accurately measuring dynamic glenohumeral joint motion under in vivo conditions. The model-based technique achieves accuracy levels that far surpass all previously reported non-invasive techniques for measuring in vivo glenohumeral joint motion. This technique is supported by a rigorous validation study that provides a realistic simulation of in vivo conditions and we fully expect to achieve these levels of accuracy with in vivo human testing. Future research will use this technique to analyze shoulder motion under a variety of testing conditions and to investigate the effects of conservative and surgical treatment of rotator cuff tears on dynamic joint stability. [DOI: 10.1115/1.2206199]

Keywords: shoulder, kinematics, accuracy, glenohumeral joint, rotator cuff

Introduction

The shoulder is a complex system consisting of three bones (scapula, humerus, clavicle), four joints (glenohumeral, scapulothoracic, acromioclavicular, and sternoclavicular) and a vast number of surrounding tendons and ligaments. Much of shoulder motion is accomplished by the glenohumeral joint and significant research efforts have focused on accurately measuring glenohumeral joint motion. However, accurately measuring in vivo glenohumeral joint translations and rotations during shoulder motion is a significant challenge.

Conventional approaches for measuring three-dimensional (3D) glenohumeral joint position and motion have relied upon cadaveric simulations, two-dimensional (2D) imaging, static 3D imaging, conventional motion measurement systems, and invasive techniques using bone pins. Unfortunately, there are significant limitations associated with each of these approaches. Cadaveric experiments [1–6] can provide highly accurate measures of joint position or motion, but are unable to accurately duplicate the complex motions, muscle forces, or joint forces associated with dynamic in vivo conditions. Glenohumeral joint position has been evaluated radiographically, using fluoroscopy to measure dynamic joint motion [7–10] or plane films to measure static joint position [11–16]. However, these 2D assessments of glenohumeral joint motion cannot sufficiently characterize motion of a joint that is capable of translating in three directions and rotating about three axes. Static 3D imaging of glenohumeral joint position has been performed with magnetic resonance imaging [17–25], CT [26], or biplane radiography [27], but these techniques are currently incapable of assessing dynamic joint motion. Conventional motion measurement systems have used video cameras to measure the position of surface markers or anatomical landmarks [28–38] or have relied on surface-mounted electromagnetic motion sensors [39–46]. Combinations of the aforementioned approaches are also used, with Barnett and colleagues describing the combined use of a surface-mounted scapular locator, electromagnetic device, and

optical motion tracking system [47]. Skin-mounted sensors are highly susceptible to skin movement artifact, and their reliability for the accurate assessment of glenohumeral joint kinematics has not been established. Invasive techniques using bone pins have been used by McClure and colleagues to directly measure scapular motion of eight volunteers [48]. However, this invasive approach not only limits the number of willing volunteers, but also makes serial studies over time impractical since bone pins cannot be reliably secured in the same location. More recently, our laboratory has begun using dynamic radiostereometric analysis (RSA) to measure 3D glenohumeral joint kinematics by tracking the position of implanted tantalum beads with a novel, high-speed, biplane x-ray system. This approach has been used extensively to study in vivo knee kinematics in canines [49,50] and humans [51]. However, tantalum marker implantation is an invasive procedure and therefore is limited to only those subjects who are undergoing a surgical procedure.

To overcome the limitations associated with existing methods for measuring glenohumeral joint motion, our laboratory has developed a new technique for measuring 3D joint kinematics. This technique is based on the work of You and colleagues [52] and compares digitally reconstructed radiographs to biplane fluoroscopic images. The purpose of this study was to compare a new model-based tracking technique for measuring 3D glenohumeral joint kinematics to a well-established, accurate dynamic RSA technique that measures joint kinematics by tracking the position of implanted tantalum beads [49]. Based on preliminary testing, we hypothesized that the model-based tracking technique would track the 3D position and orientation of the humerus and scapula to within 0.5 mm and 1.0 deg of the dynamic RSA technique.

Methods

Overview. We have developed a technique for accurately measuring in vivo joint motion from biplane radiographic images that does not require implanted tantalum beads. This technique— referred to as the model-based tracking technique—tracks the position of bones based on their 3D shape and texture. To validate this technique, we: (1) implanted tantalum beads into the humerus and scapula of cadaver specimens, (2) recorded biplane radiographic images of the shoulder while manually moving the specimen's arm, (3) measured the position of the humerus and scapula using the model-based tracking system, (4) measured the position of the humerus and scapula by tracking the implanted tantalum beads with dynamic RSA, and then (5) compared the results of the two techniques. The RSA data were used as the "gold standard."

Specimen Preparation. Accuracy tests should resemble actual testing conditions to the greatest extent possible to recreate imaging conditions, movement speeds, and other factors that may influence measurement accuracy. To provide a realistic simulation of the in vivo condition, we obtained three intact, fresh-frozen cadaver torsos (age: 89.0 ± 6.2). Tantalum beads 1.6 mm in diameter were implanted into the humerus and scapula of both shoulders. For the humerus, four markers were inserted through the greater tuberosity and widely distributed throughout the humeral head. For the scapula, markers were implanted into the acromion, scapular spine, glenoid neck, and coracoid process. The instruments for implanting the markers consisted of matched stainless steel cannulas, inserts, and drill guides with depth stops. The cannula/insert was used to drill a 2 mm hole (through skin and bone) at the proper angle and to the proper depth. The insert was removed and a bead was inserted into the cannula (surrounded by bone wax) and pushed to the end of the hole. A nylon cord was secured to the elbow so that shoulder motion could be manually simulated via a pulley system.

Testing Setup. Specimens were secured to a custom testing apparatus and positioned with the glenohumeral joint centered in the biplane x-ray system. The biplane x-ray system consists of two

100 kW pulsed x-ray generators (EMD Technologies CPX 3100CV) and two 30 cm image intensifiers (Shimadzu Medical Systems, model AI5765HVP), optically coupled to synchronized high-speed video cameras (Phantom IV, Vision Research) configured in a custom gantry to enable a variety of motion studies. The system is configured with a 60 deg inter-beam angle, an x-ray source-to-object distance of 105 cm, and object-to-intensifier distance of 75 cm.

Testing Procedures. Three shoulder motions (involving both glenohumeral and scapulothoracic motion) were simulated: frontal-plane elevation, sagittal-plane elevation, and external rotation. These motions approximately represented rotations about a medial/lateral axis, an anterior/posterior axis, and a superior/inferior axis centered on the glenoid. For each shoulder we conducted three trials for the elevation motions and two trials for the rotation motions. Thus, a total of 16 motion trials per specimen (eight per shoulder) were conducted and analyzed. It was not necessary to reproducibly create a particular motion since the model-based tracking measurements were compared with the RSA measurements within each trial. All radiographic images were acquired with the x-ray generators in continuous radiographic mode (70 kV, 320 mA). The x-ray images were acquired at 50 frames/s with the video cameras shuttered at 1/500 s to eliminate motion blur.

After testing was completed, we obtained a CT image of the cadaveric shoulders. The scans were performed on a LightSpeed16 system (GE Medical Systems), in axial mode with 1.25 mm slice spacing, 18 cm field of view and 512×512 pixel image size (in-plane resolution of 0.35 mm).

Measuring Joint Position With Model-Based Tracking. The model-based tracking technique is based on the following concept: given the geometry of the biplane x-ray system and a 3D bone model (from a CT scan), a pair of digitally reconstructed radiographs (DRRs) can be generated via ray-traced projection through the 3D bone model (Fig. 1). By optimizing the similarity between the two DRRs and the actual 2D biplane radiographic images, the in vivo position and orientation of a given bone can be estimated. Sobel edge-detector output is added to the base images for both the DRRs and the radiographs to enhance the matching process. Match quality is measured by calculating the correlation coefficient of each DRR with its corresponding radiograph, then multiplying the two view correlations to get total system correlation.

The first step in the model-based tracking involved developing the 3D volumetric bone model. First, the humerus and scapula CT images were manually segmented from other bones and soft tissue. The implanted tantalum beads were manually removed from the CT images so that the presence of implanted beads did not improve the model-based tracking in any way. The CT volume was then interpolated using a feature-based interpolation technique and scaled to have cubic voxels with dimensions similar to the 2D pixel size in the biplane x-ray system images.

The model-based tracking process is performed with an operator-friendly workbench of graphical tools designed by the authors. This workbench includes the following tools: (1) a visual overlay of the DRRs on the radiographs that facilitates the operator's initial guesses and provides contrasting colors to help the operator match position and orientation, (2) an array of six slider bars that control the position and orientation of the model, (3) a low-resolution 2D search tool that performs a wide-latitude, exhaustive search by translating and rotating each DRR to maximize the correlation with its radiograph, (4) a high-resolution (but narrow latitude) six-axis search tool to refine position and orientation, (5) a linear-projection tool that uses the solution from two successive frames to calculate a starting guess for the next frame and then optimizes the solution with the 2D and six-axis search tools, (6) tools for charting the motion and visualizing a movie of successive frames to help the operator evaluate the quality of the
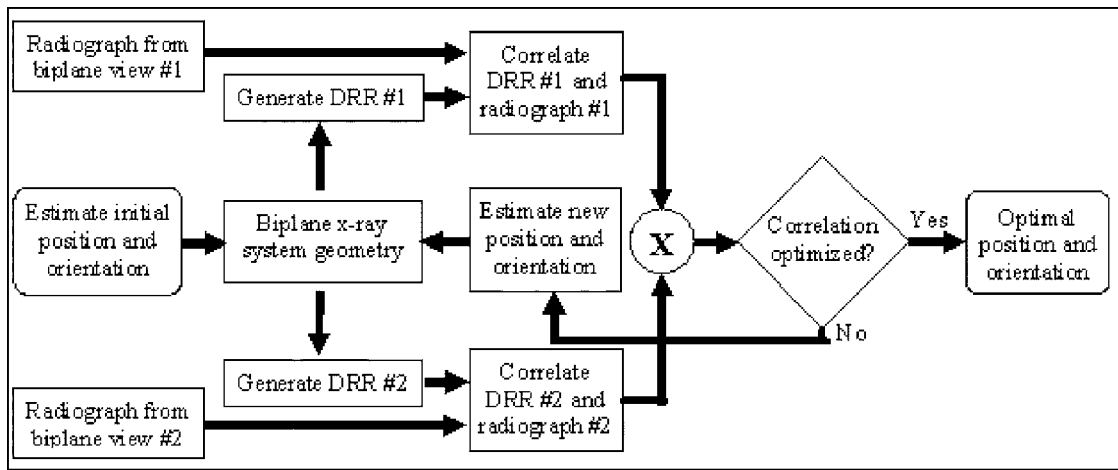
Fig. 1 Flow chart showing the process used by the model-based tracking algorithm to find a bone's optimal position and orientation from a pair of biplane x-ray images

automated solution, and (7) an interpolation tool that corrects poor quality solution frames by calculating linear, quadratic, or cubic interpolations based on frames with known good solutions.

Initial estimates for bone position and orientation were obtained by manually adjusting the six motion parameters (three positions, three rotations) to obtain a good visual match between fluoroscopic images and DRRs for both biplane views (Fig. 1). The program measured the quality of the initial guess by generating a DRR for each of the biplane views (Fig. 2), enhancing each view by adding a Sobel edge detector output to the original DRR, calculating the correlation coefficient of each DRR with its corresponding radiograph, and multiplying the two correlation coefficients to get a system-correlation measure. The initial guess was improved using the low-resolution 2D search tool that iterated several (typically 2–10) times until the correlation stopped improving. The solution was further refined with the high-resolution six-axis search tool which determined the six-coordinate gradient of the correlation product with finite differences and performed a

quadratic search along the gradient line for the maximum correlation product. This process was repeated until the new guess changed by less than 0.1 mm and 0.1 deg for three successive iterations. Initial guesses were made manually for the first two frames in each motion sequence. Since the rapid frame rate minimized differences in joint position between frames, the initial guess for each successive frame was obtained by making a linear projection from the solution of the previous two frames. Thus, the final solution of the previous two frames was used to provide an initial starting point for the subsequent frame. Tracking for the remainder of the motion sequence proceeded without additional user interaction.

The tracking workbench program was accelerated by parallelizing its calculations on a cluster of 13 inexpensive microcomputers (3.4 GHz Pentium 4, Silicon Mechanics iServ R100, Seattle, WA) linked by a gigabit Ethernet switch. This decreased the time required to track a scapula from approximately 8 h on a single personal computer (3.4 GHz Pentium 4) to approximately 40 min on the parallel processing system. For a typical trial, each frame of data requires approximately 40–50 s of computing time for the solution to converge. The operator's workstation controls the search processes with a parallel state-machine algorithm, but delegates the computation-intensive DRR projection, edge enhancement, and correlation calculations to the 12 worker nodes. The nodes are scheduled dynamically using standard multiphonon ionization (MPI) protocols. Results are consolidated and presented graphically by the operator's workstation.

Using this model-based tracking technique, the 3D position and orientation of the humerus and scapula were determined independently for all frames of each trial. The final step involved determining the position of the tantalum beads within the CT bone model and then expressing their 3D position relative to a fixed laboratory coordinate system. These data enabled a direct comparison between marker-based and model-based tracking results.

Measuring Joint Position With Dynamic RSA. For comparison, the 3D position of each implanted tantalum bead was also determined from the biplane images using an established procedure that was developed and validated in our laboratory [49]. This procedure has been used extensively to measure knee kinematics in humans and canines [49–51]. The process for moving from digital biplane radiographs to 3D bead coordinates involved image distortion and nonuniformity correction, automated detection of beads from x-ray images, 2D bead centroid calculations, interactive 3D tracking and low-pass filtering [49]. This process determined the 3D location of each tantalum bead relative to the same laboratory coordinate system used by the model-based tracking
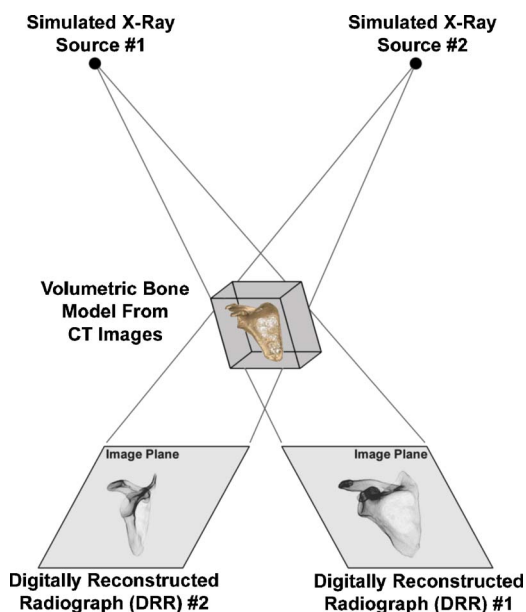
Fig. 2 A pair of digitally reconstructed radiographs (DRRs) are constructed from the CT bone model. The position and orientation of the CT bone model is refined to optimize the correlation between the two DRRs and the two biplane x-ray images.

Table 1 Measurement bias (i.e., average difference between model-based tracking and dynamic RSA) and static measurement precision (i.e., standard deviation of the difference between model-based tracking and dynamic RSA). All data are expressed relative to a laboratory-fixed coordinate system.

	Measurement bias		Dynamic measurement precision	
Axis	Scapula	Humerus	Scapula	Humerus
X	0.163±0.210 mm	0.079±0.224 mm	0.130±0.058 mm	0.077±0.033 mm
Y	−0.126±0.283 mm	−0.005±0.136 mm	0.123±0.054 mm	0.095±0.043 mm
Z	0.199±0.204 mm	−0.022±0.123 mm	0.060±0.014 mm	0.067±0.022 mm

technique. This RSA approach for measuring the position of implanted tantalum beads has been shown to be accurate to within ±0.1 mm [49].

Comparison of Techniques. To characterize the performance of the model-based tracking technique relative to dynamic RSA, accuracy was quantified in terms of bias and precision [49,53]. Measurement bias was assessed by determining the average difference in 3D bead locations between the two techniques across all trials. It was assumed that the beads were rigidly fixed in bone and that there was no motion of the beads relative to the bone during the trials. Thus, frame-to-frame variations in the reported bead locations provided a direct estimate of the uncertainty in the model-based tracking measurements independent of shoulder motion. Dynamic precision was assessed by determining the standard deviation of the difference between the two techniques during the motion trials. Finally, to provide a single measure of accuracy, we assessed the overall dynamic accuracy of the model-based tracking technique by computing the rms error between the two techniques across all trials.

We estimated rotational error by computing the effect of the maximum radial rms error on local (i.e., bone-based) coordinate system alignment. This was accomplished by computing the arctangent of the ratio of maximum radial error to the distance between the two closest anatomical landmarks used in defining each bone's local coordinate system [54]. For the humerus, this error was based on an estimated distance of 65 mm between the medial and lateral epicondyles. For the scapula, this error was based on an estimated distance of 135 mm between the angulus acromialis and the trigonum scapulae landmarks. These computed values were assumed to represent an upper bound of rotational error.

Results

The model-based tracking technique produced results that were in excellent agreement with the RSA technique. In particular, the position and orientation of the scapula and humerus were qualitatively acceptable when superimposed over the original biplane images (Fig. 3). Quantitatively measurement bias ranged from −0.126 to 0.199 mm (depending on coordinate axis) for the scapula and ranged from −0.022 to 0.079 mm for the humerus

(Table 1). Dynamic measurement precision was better than 0.130 mm for the scapula and 0.095 mm for the humerus (Table 1). Finally, the assessment of overall dynamic accuracy indicated that rms errors in any one direction were less than 0.385 mm for the scapula and less than 0.374 mm for the humerus (Table 2). These errors correspond to rotational inaccuracies of approximately 0.25 deg for the scapula and 0.47 deg for the humerus.

Discussion

The purpose of this study was to compare a new model-based tracking technique for measuring 3D glenohumeral joint kinematics to a well-established, accurate dynamic RSA technique. The results indicate that the new model-based tracking technique is accurate to within approximately ±0.5 mm of a high accuracy, validated dynamic RSA technique. In addition, the reported data indicate that this technique has low measurement bias and high measurement precision for dynamic motions.

Accurately measuring in vivo glenohumeral joint motion is important for understanding, among other things, the etiology of rotator cuff injuries. For instance, superior translation of the humerus relative to the glenoid is widely believed to decrease the subacromial space—i.e., the space between the humerus and the acromion occupied by the rotator cuff's supraspinatus tendon—and cause pathologic contact between the supraspinatus tendon and acromion. This phenomenon, known as subacromial impingement, is widely believed to contribute significantly to the development of rotator cuff tears [55]. The subacromial space has been reported to be approximately 5–8 mm, depending on gender and arm position [21]. Thus, a 1–2 mm increase in superior glenohumeral translation may be clinically significant since it potentially represents a 12–40% decrease in subacromial space. The technique reported here is capable of detecting changes in joint position within this clinically significant level (i.e., 1–2 mm). Specifically, a rms error of 0.4 mm corresponds to approximately 4% to 8% of the subacromial space thickness. Without a sufficiently accurate measuring system, the sample size necessary to detect statistically significant differences in in vivo glenohumeral joint motion would be prohibitive.

Fig. 3 Single-frame model-based tracking solution for the scapula (left) and humerus (right). In each image, the two digitally reconstructed radiographs (DRRs)—i.e., the highlighted bones in each image—are superimposed over the original pair of biplane x-ray images in the position and orientation that maximized the correlation between the DRRs and biplane x-ray images. Note that the implanted tantalum beads, which are visible in the fluoroscopic images, have been removed from the volumetric CT bone model and thus do not appear in the DRRs.

Table 2 Average rms errors (± st. dev.) between the model-based tracking and RSA techniques. Results are expressed in a laboratory-based coordinate system.

Axis	Scapula	Humerus
X	0.288±0.166 mm	0.374±0.151 mm
Y	0.385±0.134 mm	0.305±0.101 mm
Z	0.354±0.126 mm	0.217±0.113 mm
Radial	0.597±0.184 mm	0.530±0.192 mm

Previous efforts aimed at measuring in vivo shoulder motion have relied largely upon conventional techniques such as electromagnetic motion sensors and video analysis of skin markers. The differences in reported glenohumeral joint motion between these various measurement techniques can be significant. For example, Tibone and colleagues used a skin-mounted electromagnetic motion sensor to measure anterior glenohumeral translation during an anteroposterior drawer examination of the shoulder. In 16 female swimmers, the authors reported average anteroposterior translations of 12.4 mm in the dominant arm and 13.8 mm in the non-dominant arm [45]. By comparison, Tillander and Norlin used an invasive device that consisted of a sliding ruler whose ends were rigidly attached to the humerus and glenoid to report intraoperative measures of anterior glenohumeral translation in 58 patients undergoing shoulder surgery. The average anterior translation for patients whose shoulders were described clinically as stable was 5 mm [56]. For further comparison, Brenneke and colleagues performed a cadaveric study that measured anterior glenohumeral translation with a motion measurement system that was rigidly attached the humerus and glenoid. They reported that the humerus translated 8–25 mm relative to the glenoid during clinical examinations [57]. The data from these three studies suggest that anterior humeral head translation may range from 5 to 25 mm. To help understand the significance of these reported translations, the anterior-posterior dimension of the glenoid, measured in 140 shoulders, has been reported to be 29±3.2 mm [58]. Thus, reporting that the humerus translates anteriorly greater than 15 mm (i.e., half of the anterior-posterior dimension) suggests that the joint approaches full dislocation during a simulated clinical exam. This seems highly unlikely. Although the wide range of translations reported in these studies certainly reflects, to some extent, differences in testing protocols, it more importantly highlights limitations associated with previous studies and emphasizes the need for a technique that accurately measures in vivo glenohumeral joint motion during shoulder motion.

It is important to recognize that in vivo accuracy has not been assessed for the vast majority of studies using conventional techniques to measure shoulder motion. However, a very limited number of studies have reported measures of in vivo accuracy. Karduna and colleagues reported errors in scapular kinematics by comparing measurements from a skin-mounted electromagnetic motion sensor to a sensor rigidly mounted to the scapula via bone pins [59]. The average rms errors from 0 to 150 deg of humerothoracic motion ranged from 1.1 to 11.4 deg. However, these errors varied greatly between specific motions and tended to be much greater above 120 deg, i.e., the position associated with overhead activities where pain and disability due to rotator cuff impingement is greatest. In a similar study, Meskers and colleagues assessed the static measurement repeatability of an electromagnetic tracking device by comparing its measurements to those recorded with a spatial linkage digitizer [60]. The authors reported translational errors of 1.58, 2.07, and 2.64 mm in the x, y, and z directions, and rotational errors of scapular and humeral orientation that varied from 1.12 to 5.07 deg. Given the clinical significance of small (i.e., 1–2 mm) changes in glenohumeral

joint position, previous studies have not provided sufficiently accurate, 3D measurements of in vivo glenohumeral joint motion during dynamic shoulder motion.

Similar techniques have been developed for measuring in vivo joint motion from fluoroscopic images, but these techniques have either relied upon single-plane radiographic systems where errors parallel to the imaging beam are large [61] or have been limited to the analysis of static activities [62]. Perhaps more importantly, the validation studies supporting the use of these techniques have not accurately represented the challenges associated with the in vivo analysis of bone motion. Specifically, the validation studies have used phantom objects that do not duplicate complex bone geometries [62] or have relied upon validation based on the tracking of metal implants where edges are clearly defined [63].

In summary, this model-based tracking approach represents a non-invasive technique for accurately measuring dynamic glenohumeral joint motion that does not require the implantation of tantalum beads. The model-based technique achieves accuracy levels that far surpass all previously reported non-invasive techniques for measuring in vivo glenohumeral joint motion. This technique is supported by a rigorous validation study that provides a realistic simulation of in vivo conditions and we fully expect to achieve these levels of accuracy with in vivo patient testing. Future research will use this technique to analyze shoulder motion under a variety of testing conditions (e.g., during rehabilitation exercises or pitching) and to investigate the effects of conservative and surgical treatment of rotator cuff tears on dynamic joint stability.

References

[1] Debski, R. E., McMahon, P. J., Thompson, W. O., Woo, S. L., Warner, J. J., and Fu, F. H., 1995, "A New Dynamic Testing Apparatus to Study Glenohumeral Joint Motion," J. Biomech., **28**(7), pp. 869–74.

[2] Halder, A. M., Zhao, K. D., Odriscoll, S. W., Morrey, B. F., and An, K. N., 2001, "Dynamic Contributions to Superior Shoulder Stability," J. Orthop. Res., **19**(2), pp. 206–212.

[3] Payne, L. Z., Deng, X. H., Craig, E. V., Torzilli, P. A., and Warren, R. F., 1997, "The Combined Dynamic and Static Contributions to Subacromial Impingement. A Biomechanical Analysis," Am. J. Sports Med., **25**(6), pp. 801–808.

[4] Sharkey, N. A., and Marder, R. A., 1995, "The Rotator Cuff Opposes Superior Translation of the Humeral Head," Am. J. Sports Med., **23**(3), pp. 270–275.

[5] Wuelker, N., Schmotzer, H., Thren, K., and Korell, M., 1994, "Translation of the Glenohumeral Joint With Simulated Active Elevation," Clin. Orthop. Relat. Res., **309**, pp. 193–200.

[6] Wuelker, N., Wirth, C. J., Plitz, W., and Roetman, B., 1995, "A Dynamic Shoulder Model: Reliability Testing and Muscle Force Study," J. Biomech., **28**(5), pp. 489–499.

[7] Burkhart, S. S., 1992, "Fluoroscopic Comparison of Kinematic Patterns in Massive Rotator Cuff Tears. A Suspension Bridge Model," Clin. Orthop. Relat. Res., **284**, pp. 144–152.

[8] Mandalidis, D. G., Mc Glone, B. S., Quigley, R. F., McInerney, D., and O'Brien, M., 1999, "Digital Fluoroscopic Assessment of the Scapulohumeral Rhythm," Surg. Radiol. Anat., **21**(4), pp. 241–246.

[9] Pfirrmann, C. W., Huser, M., Szekely, G., Hodler, J., and Gerber, C., 2002, "Evaluation of Complex Joint Motion With Computer-Based Analysis of Fluoroscopic Sequences," Invest. Radiol., **37**(2), pp. 73–76.

[10] Werner, C. M., Nyffeler, R. W., Jacob, H. A., and Gerber, C., 2004, "The Effect of Capsular Tightening on Humeral Head Translations," J. Orthop. Res., **22**(1), pp. 194–201.

[11] Chen, S. K., Simonian, P. T., Wickiewicz, T. L., Otis, J. C., and Warren, R. F., 1999, "Radiographic Evaluation of Glenohumeral Kinematics: A Muscle Fatigue Model," J. Shoulder Elbow Surg., **8**(1), pp. 49–52.

[12] Deutsch, A., Altchek, D. W., Schwartz, E., Otis, J. C., and Warren, R. F., 1996, "Radiologic Measurement of Superior Displacement of the Humeral Head in the Impingement Syndrome," J. Shoulder Elbow Surg., **5**(3), pp. 186–193.

[13] Hawkins, R. J., Schutte, J. P., Janda, D. H., and Huckell, G. H., 1996, "Translation of the Glenohumeral Joint With the Patient Under Anesthesia," J. Shoulder Elbow Surg., **5**(4), pp. 286–292.

[14] Howell, S. M., Galinat, B. J., Renzi, A. J., and Marone, P. J., 1988, "Normal and Abnormal Mechanics of the Glenohumeral Joint in the Horizontal Plane," J. Bone Jt. Surg., Am. Vol., Vol. **70**(2), pp. 227–32.

[15] Poppen, N. K., and Walker, P. S., 1976, "Normal and Abnormal Motion of the Shoulder," J. Bone Jt. Surg., Am. Vol., Vol. **58**(2), pp. 195–201.

[16] Yamaguchi, K., Sher, J. S., Andersen, W. K., Garretson, R., Uribe, J. W., Hechtman, K., and Neviaser, R. J., 2000, "Glenohumeral Motion in Patients With Rotator Cuff Tears: A Comparison of Asymptomatic and Symptomatic Shoulders," J. Shoulder Elbow Surg., **9**(1), pp. 6–11.

[17] Beaulieu, C. F., Hodge, D. K., Bergman, A. G., Butts, K., Daniel, B. L., Napper, C. L., Darrow, R. D., Dumoulin, C. L., and Herfkens, R. J., 1999,

"Glenohumeral Relationships During Physiologic Shoulder Motion and Stress Testing: Initial Experience With Open MR Imaging and Active Imaging-Plane Registration," Radiology, **212**(3), pp. 699–705.

[18] Cardinal, E., Buckwalter, K. A., and Braunstein, E. M., 1996, "Kinematic Magnetic Resonance Imaging of the Normal Shoulder: Assessment of the Labrum and Capsule," Can. Assoc. Radiol. J., **47**(1), pp. 44–50.

[19] Graichen, H., Bonel, H., Stammberger, T., Englmeier, K. H., Reiser, M., and Eckstein, F., 1999, "Subacromial Space Width Changes During Abduction and Rotation—A 3-D MR Imaging Study," Surg. Radiol. Anat., **21**(1), pp. 59–64.

[20] Graichen, H., Stammberger, T., Bonel, H., Karl-Hans, E., Reiser, M., and Eckstein, F., 2000, "Glenohumeral Translation During Active and Passive Elevation of the Shoulder—A 3D Open-MRI Study," J. Biomech., **33**(5), pp. 609–613.

[21] Graichen, H., Bonel, H., Stammberger, T., Englmeier, K. H., Reiser, M., and Eckstein, F., 2001, "Sex-Specific Differences of Subacromial Space Width During Abduction, With and Without Muscular Activity, and Correlation With Anthropometric Variables," J. Shoulder Elbow Surg., **10**(2), pp. 129–135.

[22] Graichen, H., Stammberger, T., Bonel, H., Wiedemann, E., Englmeier, K. H., Reiser, M., and Eckstein., F., 2001, "Three-Dimensional Analysis of Shoulder Girdle and Supraspinatus Motion Patterns in Patients With Impingement Syndrome," J. Orthop. Res., **19**(6), pp. 1192–1198.

[23] Rhoad, R. C., Klimkiewicz, J. J., Williams, G. R., Kesmodel, S. B., Udupa, J. K., Kneeland, J. B., and Iannotti, J. P., 1998, "A New In Vivo Technique for Three-Dimensional Shoulder Kinematics Analysis," Skeletal Radiol., **27**(2), pp. 92–97.

[24] Solem-Bertoft, E., Thuomas, K. A., and Westerberg, C. E., 1993, "The Influence of Scapular Retraction and Protraction on the Width of the Subacromial Space. An MRI Study," Clin. Orthop. Relat. Res., **296**, pp. 99–103.

[25] von Eisenhart-Rothe, R. M., Jager, A., Englmeier, K. H., Vogl, T. J., and Graichen, H., 2002, "Relevance of Arm Position and Muscle Activity on Three-Dimensional Glenohumeral Translation in Patients With Traumatic and Atraumatic Shoulder Instability," Am. J. Sports Med., **30**(4), pp. 514–522.

[26] Baeyens, J. P., Van Roy, P., De Schepper, A., Declercq, G., and Clarijs, J. P., 2001, "Glenohumeral Joint Kinematics Related to Minor Anterior Instability of the Shoulder at the end of the Late Preparatory Phase of Throwing," Clin. Biomech. (Bristol, Avon), **16**(9), pp. 752–757.

[27] Paletta, G. A., Jr., Warner, J. J., Warren, R. F., Deutsch, A., and Altchek, D. W., 1997, "Shoulder Kinematics With Two-Plane X-Ray Evaluation in Patients With Anterior Instability or Rotator Cuff Tearing," J. Shoulder Elbow Surg., **6**(6), pp. 516–527.

[28] Barrentine, S. W., Fleisig, G. S., Whiteside, J. A., Escamilla, R. F., and Andrews, J. R., 1998, "Biomechanics of Windmill Softball Pitching With Implications About Injury Mechanisms at the Shoulder and Elbow," J. Orthop. Sports Phys. Ther., **28**(6), pp. 405–415.

[29] Davis, J. L., Growney, E. S., Johnson, M. E., Iuliano, B. A., and An, K. N., 1998, "Three-Dimensional Kinematics of the Shoulder Complex During Wheelchair Propulsion: A Technical Report," J. Rehabil. Res. Dev., **35**(1), pp. 61–72.

[30] Dillman, C. J., Fleisig, G. S., and Andrews, J. R., 1983, "Biomechanics of Pitching With Emphasis Upon Shoulder Kinematics," J. Orthop. Sports Phys. Ther., **18**(2), pp. 402–408.

[31] Doorenbosch, C. A., Mourits, A. J., Veeger, D. H., Harlaar, J., and van der Helm, F. C., 2001, "Determination of Functional Rotation Axes During Elevation of the Shoulder Complex," J. Orthop. Sports Phys. Ther., **31**(3): pp. 133–137.

[32] Escamilla, R. F., Fleisig, G. S., Zheng, N., Barrentine, S. W., and Andrews, J. R., 2001, "Kinematic Comparisons of 1996 Olympic Baseball Pitchers," J. Sports Sci., **19**(9), pp. 665–676.

[33] Fleisig, G. S., Andrews, J. R., Dillman, C. J., and Escamilla, R. F., 1995, "Kinetics of Baseball Pitching With Implications About Injury Mechanisms," Am. J. Sports Med., **23**(2), pp. 233–229.

[34] Fleisig, G. S., Barrentine, S. W., Zheng, N., Escamilla, R. F., and Andrews, J. R., 1999, "Kinematic and Kinetic Comparison of Baseball Pitching Among Various Levels of Development," J. Biomech., **32**(12), pp. 1371–1375.

[35] McCann, P. D., Wootten, M. E., Kadaba, M. P., and Bigliani, L. U., 1993, "A Kinematic and Electromyographic Study of Shoulder Rehabilitation Exercises," Clin. Orthop. Relat. Res., **288**, pp. 179–188.

[36] Murray, T. A., Cook, T. D., Werner, S. L., Schlegel, T. F., and Hawkins, R. J., 2001, "The Effects of Extended Play on Professional Baseball Pitchers," Am. J. Sports Med., **29**(2), pp. 137–142.

[37] Wang, Y. T., Ford, H. T., III, Ford, H. T., Jr., and Shin, D. M., 1995, "Three-Dimensional Kinematic Analysis of Baseball Pitching in Acceleration Phase," Percept. Mot. Skills, **80**(1), pp. 43–48.

[38] Werner, S. L., Gill, T. J., Murray, T. A., Cook, T. D., and Hawkins, R. J., 2001, "Relationships Between Throwing Mechanics and Shoulder Distraction in Professional Baseball Pitchers," Am. J. Sports Med., **29**(3), pp. 354–358.

[39] An, K. N., Browne, A. O., Korinek, S., Tanaka, S., and Morrey, B. F., 1991, "Three-Dimensional Kinematics of Glenohumeral Elevation," J. Orthop. Res., **9**(1), pp. 143–149.

[40] Borstad, J. D., and Ludewig, P. M., 2002, "Comparison of Scapular Kinematics Between Elevation and Lowering of the arm in the Scapular Plane," J. Orthop. Sports Phys. Ther., **17**(9–10), pp. 650–659.

[41] Johnson, M. P., McClure, P. W., and Karduna, A. R., 2001, "New Method to Assess Scapular Upward Rotation in Subjects With Shoulder Pathology," Cancer Commun., **31**(2), pp. 81–89.

[42] Ludewig, P. M., and Cook, T. M., 2002, "Translations of the Humerus in Persons With Shoulder Impingement Symptoms," J. Orthop. Sports Phys. Ther., **32**(6), pp. 248–259.

[43] Meskers, C. G., van der Helm, F. C., Rozendaal, L. A., and Rozing, P. M., 1998, "In Vivo Estimation of the Glenohumeral Joint Rotation Center From Scapular Bony Landmarks by Linear Regression," J. Biomech., **31**(1), pp. 93–96.

[44] Stokdijk, M., Nagels, J., and Rozing, P. M., 2000, "The Glenohumeral Joint Rotation Centre In Vivo," J. Biomech., **33**(12), pp. 1629–1636.

[45] Tibone, J. E., Lee, T. Q., Csintalan, R. P., Dettling, J., and McMahon, P. J., 2002, "Quantitative Assessment of Glenohumeral Translation," Clin. Orthop. Relat. Res., **400**, pp. 93–97.

[46] Tsai, N. T., McClure, P. W., and Karduna, A. R., 2003, "Effects of Muscle Fatigue on 3-Dimensional Scapular Kinematics," Arch. Phys. Med. Rehabil., **84**(7), pp. 1000–1005.

[47] Barnett, N. D., Duncan, R. D., and Johnson, G. R., 1999, "The Measurement of Three Dimensional Scapulohumeral Kinematics—A Study of Reliability," Clin. Biomech. (Bristol, Avon), **14**(4), pp. 287–290.

[48] McClure, P. W., Michener, L. A., Sennett, B. J., and Karduna, A. R., 2001, "Direct 3-Dimensional Measurement of Scapular Kinematics During Dynamic Movements In Vivo," J. Shoulder Elbow Surg., **10**(3), pp. 269–277.

[49] Tashman, S., and Anderst, W., 2003, "In-Vivo Measurement of Dynamic Joint Motion Using High Speed Biplane Radiography and CT: Application to Canine ACL Deficiency," ASME J. Biomech. Eng., **125**(2), pp. 238–245.

[50] Tashman, S., Anderst, W. J., Kolowich, P., Havstad, S., and Arnoczky, S. P., 2004, "Kinematics of the ACL-Deficient Canine Knee During Gait: Serial Changes Over Two Years," J. Orthop. Res., **22**(5), pp. 931–941.

[51] Tashman, S., Collon, D., Anderson, K., Kolowich, P., and Anderst, W., 2004, "Abnormal Rotational Knee Motion During Running After Anterior Cruciate Ligament Reconstruction," Am. J. Sports Med., **32**(4), pp. 975–983.

[52] You, B. M., Siy, P., Anderst, W., and Tashman, S., 2001, "In Vivo Measurement of 3-D Skeletal Kinematics From Sequences of Biplane Radiographs: Application to Knee Kinematics," IEEE Trans. Med. Imaging, **20**(6), pp. 514–525.

[53] ASTM, 1996, *Standard Practice for Use of the Terms Precision and Bias in ASTM Test Methods*, West Conshohocken, PA.

[54] Wu, G., van der Helm, F. C., Veeger, H. E., Makhsous, M., Van Roy, P., Anglin, C., Nagels, J., Karduna, A. R., McQuade, K., Wang, X., Werner, F. W., and Buchholz, B., 2005, "ISB Recommendation on Definitions of Joint Coordinate Systems of Various Joints for the Reporting of Human Joint Motion—Part II: Shoulder, Elbow, Wrist and Hand," J. Biomech., **38**(5), pp. 981–992.

[55] Neer, C. S., II, 1983, "Impingement Lesions," Clin. Orthop. Relat. Res., **173**, pp. 70–77.

[56] Tillander, B., and Norlin, R., 2001, "Intraoperative Measurement of Shoulder Translation," J. Shoulder Elbow Surg., **10**(4), pp. 358–364.

[57] Brenneke, S. L., Reid, J., Ching, R. P., and Wheeler, D. L., 2000, "Glenohumeral Kinematics and Capsulo-Ligamentous Strain Resulting From Laxity Exams," Clin. Biomech. (Bristol, Avon), **15**(10), pp. 735–742.

[58] Iannotti, J. P., Gabriel, J. P., Schneck, S. L., Evans, B. G., and Misra, S., 1992, "The Normal Glenohumeral Relationships. An Anatomical Study of One Hundred and Forty Shoulders," J. Bone Jt. Surg., Am. Vol., **74**(4), pp. 491–500.

[59] Karduna, A. R., McClure, P. W., Michener, L. A., and Sennett, B., 2001, "Dynamic Measurements of Three-Dimensional Scapular Kinematics: A Validation Study," ASME J. Biomech. Eng., **123**(2), pp. 184–190.

[60] Meskers, C. G., Fraterman, H., van der Helm, F. C., Vermeulen, H. M., and Rozing, P. M., 1999, "Calibration of the "Flock of Birds" Electromagnetic Tracking Device and Its Application in Shoulder Motion Studies," J. Biomech., **32**(6), pp. 629–633.

[61] Mahfouz, M. R., Komistek, R. D., Dennis, D. A., and Hoff, W. A., 2004, "In Vivo Assessment of the Kinematics in Normal and Anterior Cruciate Ligament-Deficient Knees," J. Bone Jt. Surg., Am. Vol., **86-A**(2), pp. 56–61.

[62] Li, G., Wuerz, T. H., and DeFrate, L. E., 2004, "Feasibility of Using Orthogonal Fluoroscopic Images to Measure In Vivo Joint Kinematics," ASME J. Biomech. Eng., **126**(2), pp. 314–318.

[63] Walker, S. A., Hoff, W., Komistek, R., and Dennis, D., 1996, " 'In Vivo' Pose Estimation of Artificial Knee Implants Using Computer Vision," Biomed. Sci. Instrum., **32**, pp. 143–150.